THE JOURNAL OF PHYSICAL CHEMISTRY B

Article

pubs.acs.org/JPCB

Thermodynamic and Spectroscopic Identification of Guest Gas Enclathration in the Double Tetra-*n*-butylammonium Fluoride Semiclathrates

Seungmin Lee,[†] Youngjun Lee,[‡] Sungwon Park,[‡] Yunju Kim,[‡] Ju Dong Lee,[†] and Yongwon Seo*[,‡]

[†]Green Technology Center, Korea Institute of Industrial Technology, Ulsan 681-802, Republic of Korea

[‡]School of Urban and Environmental Engineering, Ulsan National Institute of Science and Technology, Ulsan 689-798, Republic of Korea

ABSTRACT: The precise nature and unique pattern of the double tetra-*n*-butylammonium fluoride (TBAF) semiclathrates with a guest gas (CH_4 or CO_2) was closely investigated through thermodynamic and spectroscopic analyses. The three-phase equilibria of semiclathrate (H), liquid water (L_W), and vapor (V) for the ternary CH_4 + TBAF + water and CO_2 + TBAF + water mixtures with various TBAF concentrations were experimentally measured in order to determine the stability conditions of the double TBAF semiclathrates. The double CH_4 (or CO_2) + TBAF semiclathrates showed remarkably enhanced thermal stability when compared with pure CH_4 (or CO_2) hydrate. The highest stabilization effect was observed at the stoichiometric concentration of pure TBAF semiclathrate, which is 3.3 mol %. Gas uptake measurements were undertaken in order to estimate the amount of gas consumed during double semiclathrate formation. CH_4 was found to be a relatively more favorable guest for the 5^{12} cages of the double TBAF semiclathrate than CO_2. From the results of the NMR and Raman spectroscopic analyses it was identified that the guest gas molecules (CH_4 or CO_2) were enclathrated in the 5^{12} cages of the double TBAF semiclathrates. The overall results given in this study are useful for understanding the fundamental guest gas enclathration behavior in the double semiclathrates.

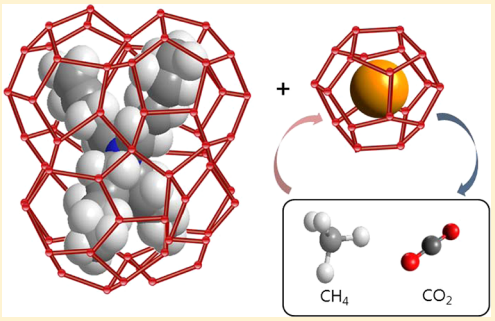

INTRODUCTION

Gas hydrates are inclusion compounds formed when guest molecules of suitable size and shape are incorporated in well-defined cages in the host lattice made of hydrogen-bonded water molecules.[1] In gas hydrates, guest molecules that are captured in the cages interact with water molecules through van der Waals forces.[1] Conventionally, gas hydrates have been of particular interest to oil and gas industries for application in areas such as the prevention of hydrate plugging in oil and gas pipelines and the exploitation of natural gas hydrates deposited in deep ocean sediments of continental margins or under permafrost regions.[1] Recently, it has also been suggested that gas hydrates show attractive method of storing large amounts of gas such as H_2 and natural gas in a unit volume.[2−4] In addition, it has been suggested that with the gas hydrate formation CO_2 can be readily separated from flue and fuel gas mixtures as a result of preferential occupation of CO_2 in hydrate cages.[5−9]

On the other hand, quaternary ammonium salts (QAS) such as tetra-*n*-butylammonium bromide (TBAB) and fluoride (TBAF) form semiclathrates with water molecules at atmospheric pressure.[10−12] In QAS semiclathrates, the water molecules together with anions such as Br^- and F^- build the polyhedral host framework of the cavities in which the tetra-*n*-butylammonium cations (TBA^+) are incorporated as the guest molecules. Semiclathrates share many of the same physical and structural properties as gas hydrates; however, the primary difference is that, in gas hydrates, the guest molecules are not physically bonded to the host water lattices, while in semiclathrates, the guest molecules can both form part of the host lattice and occupy cages after breaking part of the cage structure.[1,10−12] Because empty cages in QAS semiclathrates can capture small-sized gas molecules in mild conditions, QAS semiclathrates have been considered as a new gas storage and separation material.[13−17]

Among the QAS, TBAB semiclathrate has been targeted by many researchers for application in gas separation and storage because TBAB semiclathrate shows favorable stability conditions.[13−17] However, it has been reported that the TBAF semiclathrate, which is expected to have almost the same physical and structural properties as the TBAB semiclathrate, shows more enhanced thermal stability than TBAB semiclathrate when TBAF is involved in forming both pure semiclathrate with water and double semiclathrate with guest gases.[18−25] Despite the importance of the experimental data for the TBAF semiclathrates with many potential applications, only a few studies covering the phase equilibria of the double TBAF semiclathrate mainly with H_2, and some limited results of Raman spectroscopic analyses appear in the literature.[13,23−25]

Received: March 20, 2012
Revised: July 1, 2012
Published: July 9, 2012

Therefore, more methodical approaches based on thermodynamic and spectroscopic analyses should be undertaken in order to better understand guest gas enclathration behavior and structure details of the double TBAF semiclathrates, which are potentially applicable in gas storage and separation processes.

In the present study, the precise nature and unique pattern of the double TBAF semiclathrates with a guest gas (CH_4 or CO_2) were investigated with a focus on the stability conditions, gas uptake measurements, and spectroscopic analysis. These guest gases are sufficiently small to be captured in the empty cages of TBAF semiclathrates and are industrially important because CH_4 is a major component of natural gas and CO_2 is a target gas from flue and fuel gas mixtures. Thus, the phase equilibria of the double TBAF semiclathrates with a guest gas (CH_4 or CO_2) will not only be useful in estimating the formation/dissociation conditions and stability regions but also in designing a gas storage and separation process. In addition, the spectroscopic analysis and gas uptake measurement will provide valuable information about the guest gas enclathration behavior in the double TBAF semiclathrates. Therefore, the three-phase equilibria (semiclathrate (H)−liquid water (L_W)−vapor (V)) for the ternary CH_4 + TBAF + water and CO_2 + TBAF + water mixtures at four different concentrations of TBAF (0.8, 3.0, 3.3, and 5.3 mol %) were experimentally measured in order to provide the stability conditions of the double TBAF semiclathrates. The gas uptake during the double semiclathrate formation was also measured for the ternary CH_4 + TBAF + water and CO_2 + TBAF + water mixtures in order to confirm the amount of guest gas enclathrated. The pure and double semiclathrates were analyzed via NMR and Raman spectroscopy in order to examine the guest gas enclathration. Furthermore, a differential scanning calorimeter (DSC) was also used to confirm the dissociation temperature and dissociation enthalpy of the pure TBAF semiclathrate.

EXPERIMENTAL SECTION

Thermodynamic and Gas Uptake Measurements. The CH_4 and CO_2 gases used for the present study were supplied by Union Gas (Republic of Korea) and had stated purities of 99.95% and 99.99%, respectively. A TBAF solution with concentration of 75% in water was purchased from Sigma-Aldrich. Doubly distilled deionized water was used. All materials were used without further purification.

The experimental apparatus for the semiclathrate phase equilibria was specially designed to accurately measure the semiclathrate dissociation pressures and temperatures. The equilibrium cell was made of 316 stainless steel and had an internal volume of ~200 cm^3. Two sapphire windows at the front and back of the cell allowed visual observation of the phase transitions that occurred inside the equilibrium cell. The cell content was vigorously agitated using an impeller-type stirrer. A thermocouple with an accuracy of ±0.1 K for full range was inserted into the cell in order to measure the inner content. This thermocouple was calibrated using an ASTM 63C mercury thermometer (Ever Ready Thermometer) with a resolution of ±0.1 K. A pressure transducer (VPRT, Valcom, Japan) with an uncertainty of 0.02 MPa was used to measure the cell pressure. The pressure transducer was also calibrated using a Heise Bourdon tube pressure gauge (CMM-137219, 0−10 MPa range) with a maximum error of ±0.01 MPa in the full range. The experiment for the semiclathrate phase equilibrium measurements began with charging the equilibrium cell with ~80 cm^3 of TBAF solution. Before each experimental run, the equilibrium cell was flushed at least three times with CH_4 or CO_2 in order to remove any residual air. After the equilibrium cell was pressurized to the desired pressure with CH_4 or CO_2, the entire main system was slowly cooled to a temperature lower than the expected equilibrium temperature. Because of the thermal contraction, the cell pressure decreased slightly through decreasing the temperature at a cooling rate of 1 K/h. Then, an abrupt pressure depression was observed at the stage of the semiclathrate crystal growth after nucleation. When the pressure depression due to the semiclathrate formation reached a steady-state condition, the temperature increased in 0.1 K increments with sufficient time, and accordingly, the cell pressure increased with the semiclathrate dissociation. After all semiclathrates were dissociated with the increasing temperature, the cell pressure slightly increased again due to the thermal expansion. The H−L_W−V equilibrium points in each pressure condition were determined using the intersection between the semiclathrate dissociation and thermal expansion lines.

The gas uptake measurement was conducted in the same apparatus as that used for measuring the semiclathrate phase equilibria. The volumetric gas consumption was measured during the gas hydrate or double semiclathrate formation. The stirring rate was maintained at 300 rpm, which ensured the absence of external mass transfer resistance. The reactor was initially pressurized with CH_4 or CO_2 supplied from a gas cylinder and then maintained at a constant pressure by using a microflow syringe pump (ISCO, Model 500D) operated in a constant pressure mode. Under those isothermal and isobaric conditions, the experiment was conducted in a batch manner with a fixed amount of water. The reaction time was counted just after the nucleation of hydrate or semiclathrate crystals. As the system pressure decreased due to the gas hydrate or semiclathrate crystal growth, the piston of the syringe pump simultaneously moved upward to supplement the gas to the reactor in order to maintain the system pressure at constant level. The volume of the supplemented gas to the reactor was recorded at regular time intervals, and finally the moles of the gas consumed during the gas hydrate or semiclathrate formation were calculated using Pitzer correlations.[26]

Confirmation of the dissociation temperature and dissociation enthalpy of the pure TBAF semiclathrate was conducted using DSC (Q10, TA Instruments). A TBAF solution of ~3.5 × 10^{-3} cm^3 was sealed in an aluminum pan and placed in the DSC cell. The sample was cooled to 243 K at a rate of 1 K/min, and the semiclathrate was formed while the sample cooled. Then, the sample was heated to 323 K at a rate of 1 K/min to dissociate the semiclathrate. The area for the phase transition peak corresponds to the heat absorbed due to dissociation. More details of the experimental apparatus and procedure used in this study have been illustrated in previous papers.[17,27−29]

^{13}C NMR and Raman Spectroscopic Analysis. In this study, a Bruker 400 MHz solid-state NMR spectrometer was used to analyze the pure TBAF and double CH_4 + TBAF semiclathrates. The NMR spectra were recorded at 243 K and atmospheric pressure by placing the semiclathrate samples within a 4 mm o.d. Zr rotor that was loaded into the variable-temperature (VT) probe. All ^{13}C NMR spectra were recorded at a Larmor frequency of 100.6 MHz with magic angle spinning (MAS) between 2 and 4 kHz. A pulse length of 2 μs and pulse repetition delay of 10 s under proton decoupling were employed when a radio-frequency field strength of 50 kHz corresponding to 5 μs 90° pulses was used. The downfield

dx.doi.org/10.1021/jp302647c | J. Phys. Chem. B 2012, 116, 9075−9081

carbon resonance peak of adamantane, which was assigned a chemical shift of 38.3 ppm at 300 K, was used as an external chemical shift reference. The semiclathrate samples for the NMR analysis were prepared using the same apparatus as that used for the semiclathrate phase equilibrium measurement. When the semiclathrate formation was completed, the semiclathrates formed were finely powdered in a liquid nitrogen (N_2) vessel and sampled into a Zr rotor immersed in liquid N_2 to prevent semiclathrate dissociation.

For the Raman spectra of the TBAF semiclathrates, the formed semiclathrates were finely powered in the liquid N_2 vessel and pelletized into a cylindrical type (1 cm diameter and 0.5 cm height). Under atmospheric pressure conditions, the Raman spectra were obtained using a JASCO NRS-3100 Raman spectrometer (Japan) with a thermoelectrically cooled CCD detector and 1800 grooves/mm holographic grating. The excitation source was a diode-pumped solid-state laser emitting a 532 nm line, and the laser intensity was typically 7 mW. The temperature of the sample was maintained at ~170 K during measurement by controlling the flow rate of the liquid N_2 vapor. A more detailed description of the NMR and Raman analyses has been given in previous papers.[27−29]

RESULTS AND DISCUSSION

It has been reported that under atmospheric pressure conditions TBAF with water forms semiclathrate structures, where the small dodecahedral (5^{12}) cages of the semiclathrate are left vacant or partially occupied by water molecules.[21] The TBAF semiclathrate is known to have two crystal structures: one is a cubic structure with a hydration number of TBAF·29.7H_2O, and the other is a tetragonal structure with a hydration number of TBAF·32.8H_2O.[18,19,21,22] Komarov et al.[21] and Lee et al.[24] indicated that the maximum dissociation temperature for pure TBAF semiclathrates under atmospheric pressure conditions was observed at the stoichiometric concentration (3.3 mol %) of pure TBAF semiclathrate, where the hydration number is TBAF·29.7H_2O. In the present study, the dissociation temperature of the pure TBAF semiclathrate with a stoichiometric concentration was confirmed through the DSC. Figure 1 shows the dissociation process of pure TBAF semiclathrate in the DSC under atmospheric pressure conditions. The onset temperature of the endothermic peak is considered to be the dissociation temperature. The resulting dissociation temperature for the pure TBAF semiclathrate of 3.3 mol % was found to be 300.4 K, which is close to the value (300.85 K) presented in the literature.[21] For the semiclathrate with TBAF 3.3 mol %, it was found from the heat flow of DSC that there was no ice melting peak, indicating that all the water phase reacted with the TBAF to form a pure TBAF semiclathrate. The heat of dissociation for the pure TBAF semiclathrate was found to be 234.9 ± 1.5 J/g, which is also quite similar to the value in the literature.[22]

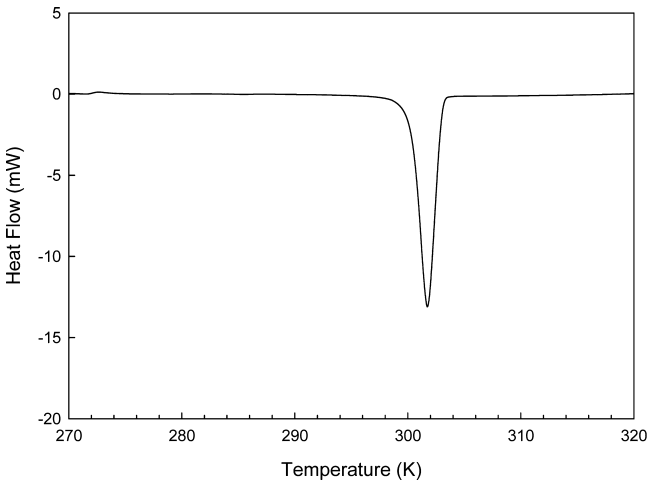

Figure 1. Dissociation process of TBAF semiclathrate in DSC under atmospheric pressure conditions.

The three-phase equilibria (H−L_W−V) for the CH_4 + TBAF + water systems were experimentally measured in order to determine the stability conditions of the double CH_4 + TBAF semiclathrates at four different TBAF concentrations of 0.8, 3.0, 3.3, and 5.3 mol %, and the overall experimental results are summarized in Table 1 and shown in Figure 2 with the three-phase equilibrium data of the pure CH_4 hydrate.[30] The H−L_W−V equilibrium conditions of the double TBAF semiclathrates were greatly shifted to the stabilized regions represented by higher temperature and lower pressure conditions when compared with the pure CH_4 hydrate system. The double CH_4 + TBAF semiclathrate systems were more stabilized when the TBAF concentration increased from 0.8 to 3.3 mol %. However, a lower stabilization effect was observed at TBAF 5.3 mol %. As can be expected from the phase diagram of the pure TBAF semiclathrate reported in the liter-

Table 1. Semiclathrate Phase Equilibrium Data for the CH_4 + TBAF + Water Systems

0.8 mol %		3.0 mol %		3.3 mol %		5.3 mol %	
T (K)	P (MPa)	T (K)	P (MPa)	T (K)	P (MPa)	T (K)	P (MPa)
294.8	2.17	302.1	2.21	302.2	2.24	298.9	2.14
295.6	3.71	302.9	3.89	302.9	3.79	299.4	3.71
296.5	5.09	303.4	5.09	303.5	5.08	299.9	4.96
297.3	6.90	304.2	7.73	304.2	7.63	300.6	7.45
298.3	9.33	304.7	9.54	304.7	9.52	300.9	9.32

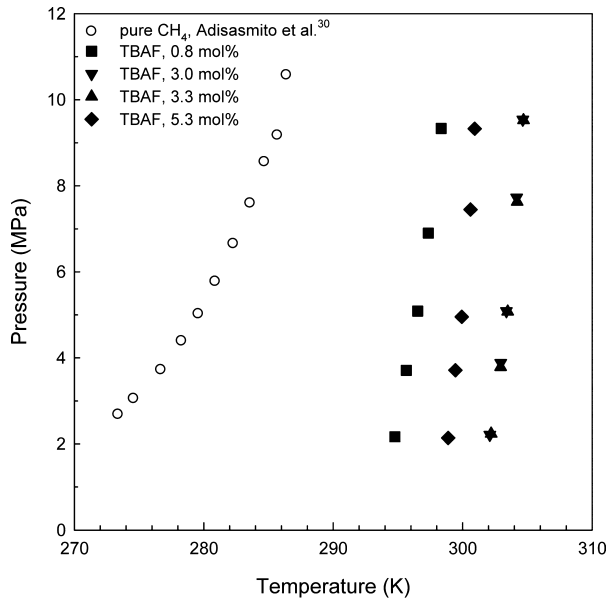

Figure 2. Semiclathrate phase equilibria of the CH_4 + TBAF + water systems.

dx.doi.org/10.1021/jp302647c | J. Phys. Chem. B 2012, 116, 9075−9081

ature,[21,24,25] for the double CH_4 + TBAF semiclathrate systems the maximum stabilization effect was observed at TBAF 3.3 mol %, which corresponds to the stoichiometric concentration of the pure TBAF semiclathrate (TBAF·29.7H_2O). For TBAF 5.3 mol %, only a stoichiometric amount of TBAF engages in the semiclathrate formation, and the remaining TBAF, which exists as free ions of TBA^+ and F^-, acts as an inhibitor rather than a semiclathrate former. Accordingly, at TBAF 5.3 mol %, the semiclathrate dissociation occurs at a higher pressure for a given temperature or at a lower temperature for a given pressure than that at TBAF 3.3 mol %. The three-phase H−L_W−V equilibria for CO_2 + TBAF + water systems showed similar trend to those for CH_4 + TBAF + water systems. The overall experimental results for the double CO_2 + TBAF semiclathrates are summarized in Table 2 and shown in Figure 3 with the

Table 2. Semiclathrate Phase Equilibrium Data for the CO_2 + TBAF + Water Systems

0.8 mol %		3.0 mol %		3.3 mol %		5.3 mol %	
T (K)	*P* (MPa)	*T* (K)	*P* (MPa)	*T* (K)	*P* (MPa)	*T* (K)	*P* (MPa)
295.0	1.55	301.4	1.57	301.5	1.59	299.5	1.61
295.4	2.51	301.6	2.40	301.7	2.36	300.0	2.31
295.7	3.51	302.0	3.09	302.0	3.10	300.1	3.07
296.0	4.44	302.2	3.94	302.2	3.92	300.3	3.85
		302.3	4.66	302.3	4.67	300.6	4.66

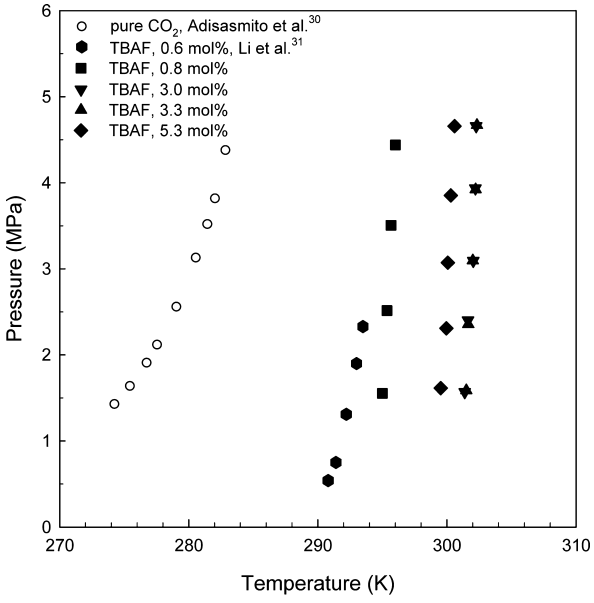

Figure 3. Semiclathrate phase equilibria of the CO_2 + TBAF + water systems.

three-phase equilibrium data of the pure CO_2 hydrate[30] and the double CO_2 + TBAF semiclathrate in the literature.[31] The presence of TBAF also led to shift of the H−L_W−V equilibrium conditions to stabilized regions when compared with the pure CO_2 hydrate. A lower stabilization effect for the double CO_2 + TBAF semiclathrates was also observed over the stoichiometric concentration of 3.3 mol %.

The gas uptake measurements were performed at constant pressure conditions in order to estimate the amount of gas consumed during the gas hydrate or semiclathrate formation. For all cases, ΔT, which is defined as the temperature difference between the equilibrium and experimental temperatures and is considered as the driving force for hydrate or semiclathrate formation, was fixed at 4.0 K. The gas consumption was monitored from the beginning of the stirring, and the reaction time was counted just after the nucleation of the hydrate or semiclathrate crystals after some induction time. The total amount of gas consumed during the formation indicates the amount of gas enclathrated in the cages of the gas hydrate or double semiclathrate and can be expressed as the value of the gas-to-water ratio, which represents the ratio of the total moles of consumed gas to the moles of initially charged water. Figure 4 shows the gas uptake curves during the formation of the pure

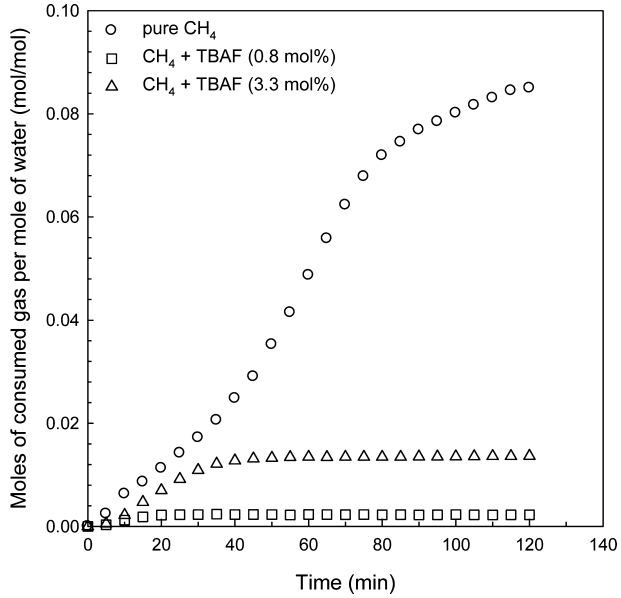

Figure 4. Gas uptake curves during the formation of the pure CH_4 hydrate and double CH_4 + TBAF semiclathrates at 8.0 MPa and ΔT = 4.0 K.

CH_4 hydrate and double CH_4 + TBAF semiclathrates at 8.0 MPa and ΔT = 4.0 K. The pure CH_4 hydrate is known to form structure I (sI) and to have the stoichiometry of CH_4·6.0H_2O.[1] Accordingly, the final value of the gas-to-water ratio for the pure CH_4 hydrate is expected to be 0.167 if it is assumed that the complete conversion of water into gas hydrate is achieved. However, in the present study the actual experimental value of the gas-to-water ratio for 2 h appeared to be lower than the expected one. This can be attributed to the limited reaction time and presence of occluded water, which is caused by the rapid growth of the hydrate crystals and as a result cannot be easily converted into a hydrate.

In pure CH_4 hydrates, CH_4 molecules can occupy both small (5^{12}) and large ($5^{12}6^2$) cages of sI while in the double CH_4 + TBAF semiclathrates, CH_4 molecules are expected to occupy only small (5^{12}) cages of semiclathrate structure.[1,21,23] Thus, as shown in Figure 4, the double CH_4 + TBAF semiclathrates showed relatively lower gas-to-water ratio values than the pure CH_4 hydrate. However, it should be noted that in the double CH_4 + TBAF semiclathrates the value of gas-to-water ratio for TBAF 0.8 mol % is remarkably lower than that for TBAF 3.3 mol %. As can be seen in Figure 1, at a stoichiometric concentration there is no remaining water phase after the TBAF semiclathrate formation, indicating that all water molecules reacted with the TBAF molecules to form the

dx.doi.org/10.1021/jp302647c | J. Phys. Chem. B 2012, 116, 9075−9081

TBAF semiclathrate; thus, there are many 5^{12} cages that can be potentially occupied by guest gas molecules such as CH_4. However, at concentrations lower than stoichiometry, a water phase must remain unreacted after the TBAF semiclathrate formation due to the relative lack of TBAF molecules, resulting in a lower amount of TBAF semiclathrates formed and, accordingly, fewer 5^{12} cages for CH_4 enclathration.

Figure 5 shows the gas uptake curves during the formation of the pure CO_2 hydrate and double CO_2 + TBAF semiclathrates

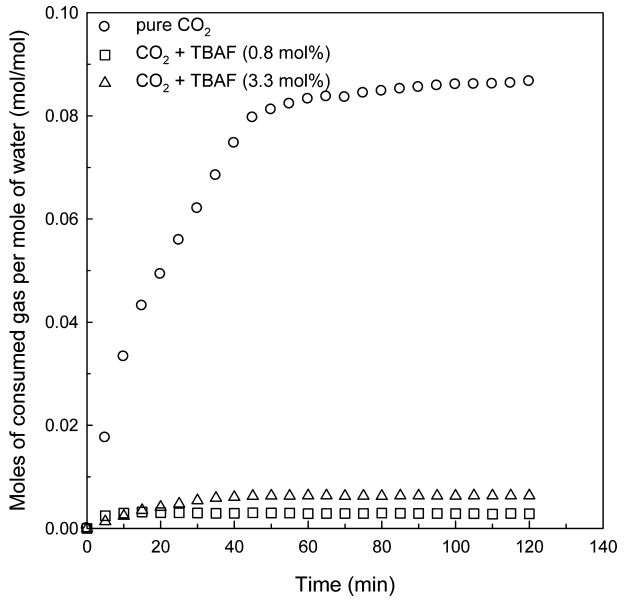

Figure 5. Gas uptake curves during the formation of the pure CO_2 hydrate and double CO_2 + TBAF semiclathrates at 3.5 MPa and ΔT = 4.0 K.

at 3.5 MPa and ΔT = 4.0 K. The double CO_2 + TBAF semiclathrates also demonstrated much lower values in the gas-to-water ratio than the pure CO_2 hydrate. From Figures 4 and 5, it should be noted that in the case of TBAF 3.3 mol % solution the accumulated amount of CO_2 enclathrated into the 5^{12} cages of the double TBAF semiclathrate was lower than that of the CH_4 during the formation of the double TBAF semiclathrates while the gas uptakes of TBAF 0.8 mol % solution for both CH_4 and CO_2 were too small to compare each other. The difference in the gas uptake can be attributed to the molecular size of guest gases. The molecular size of CO_2 is larger than that of CH_4 and is almost the same as the cavity diameter of the 5^{12} cage in the sI hydrate.[1] Accordingly, CO_2 is a relatively poor guest for the 5^{12} cages of the double TBAF semiclathrate when compared with CH_4, even though CO_2 can occupy both small and large cages of the sI hydrate. For the same reason, CO_2 shows a lower fractional occupancy of the 5^{12} cages in the sI hydrate than CH_4, resulting in a higher hydration number of $CO_2{\cdot}6.3H_2O$.[32]

In the present study, the semiclathrate samples were analyzed via ^{13}C MAS NMR to confirm the guest gas enclathration. The NMR spectroscopy has been recognized as a powerful tool for the structure identification and composition analysis of clathrates; in particular, the cage-dependent ^{13}C NMR chemical shifts for the enclathrated guest molecules can be used to determine the structure types of the formed clathrates.[33] X-ray structure analyses revealed that the crystal structure of the pure TBAF·29.7H_2O is cubic, $I\bar{4}3d$, a = 24.375(3) Å, and the structure of the pure TBAF·32.8H_2O is tetragonal, $P4_2/m$, a = 23.52 Å, c = 12.30 Å.[18,19,21,22] Sakamoto et al.[25] reported that hydrogen can be captured in the double TBAF semiclathrates through the Raman spectroscopy. However, the CH_4 gas enclathration in the double TBAF semiclathrate has not yet

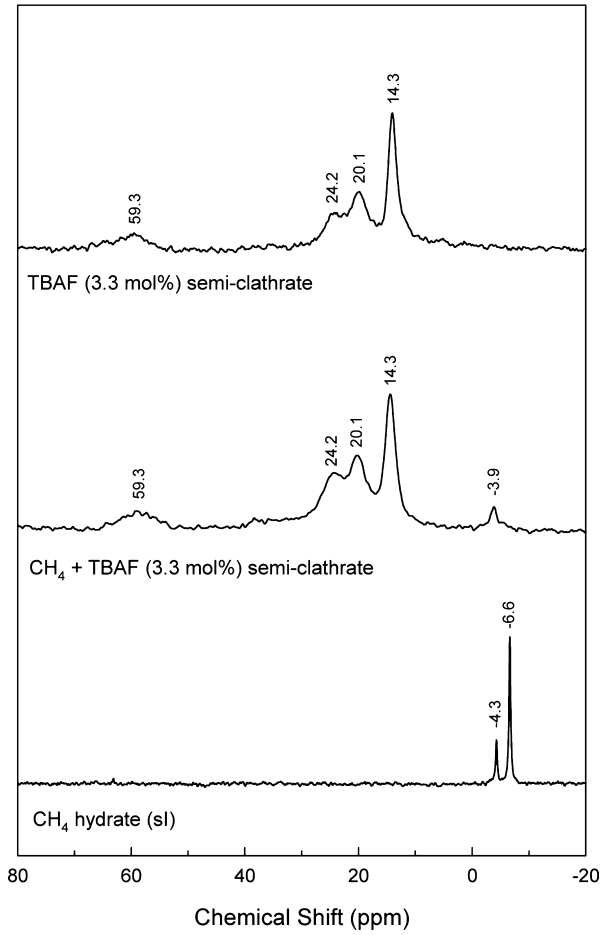

Figure 6. ^{13}C NMR spectra of the pure TBAF (3.3 mol %) semiclathrate, double CH_4 + TBAF (3.3 mol %) semiclathrate, and CH_4 hydrate.

been confirmed via NMR. Figure 6 shows a stacked plot of the ^{13}C MAS NMR spectra of a pure TBAF (3.3 mol %) semiclathrate, double CH_4 + TBAF (3.3 mol %) semiclathrate, and CH_4 hydrate. The spectrum of the CH_4 hydrate, known to form the sI, has two resonance peaks at −4.3 and −6.6 ppm. The peak at −4.3 ppm can be assigned to CH_4 molecules in the small 5^{12} cages, and the peak at −6.6 ppm can be assigned to CH_4 molecules in the large $5^{12}6^2$ cages, considering the ideal stoichiometric ratio of the small 5^{12} to the large $5^{12}6^2$ cages in the unit cell of the sI. The NMR chemical shifts of CH_4 molecules captured in sI hydrate are identical to those of literature reports.[17,27,29] On the other hand, the pure TBAF semiclathrate showed four resonance peaks at 59.3, 24.2, 20.1, and 14.3 ppm, which can be assigned to the four carbons of the *n*-butyl group of TBA^+. The double CH_4 + TBAF (3.3 mol %) semiclathrate also presented four resonance peaks at 59.3, 24.2, 20.1, and 14.3 ppm, which are the same as those from the *n*-butyl group of the pure TBAF semiclathrate. In addition, the double CH_4 + TBAF (3.3 mol %) semiclathrate additionally demonstrated one resonance peak at −3.9 ppm, which can be

dx.doi.org/10.1021/jp302647c | J. Phys. Chem. B 2012, 116, 9075−9081

assigned to the enclathrated CH_4 molecules in the 5^{12} cages of the double TBAF semiclathrate. It should be noted that in the double CH_4 + TBAB semiclathrate the resonance peak from the enclathrated CH_4 molecules was detected at −4.3 ppm, which is the same as that from the CH_4 molecules in the small 5^{12} cages of the pure CH_4 hydrate (sI).[17,27,29] When compared with the double CH_4 + TBAB semiclathrate, the slight downfield shift of the NMR signal for CH_4 molecules enclathrated in the double CH_4 + TBAF semiclathrates can be attributed to the presence of fluoride (F), which is most electronegative and thus has deshielding effect.[34]

The NMR spectra of the pure TBAF (3.0 mol %) and double CH_4 + TBAF (3.0 mol %) semiclathrates were also measured and presented in Figure 7. Each chemical shift from the pure

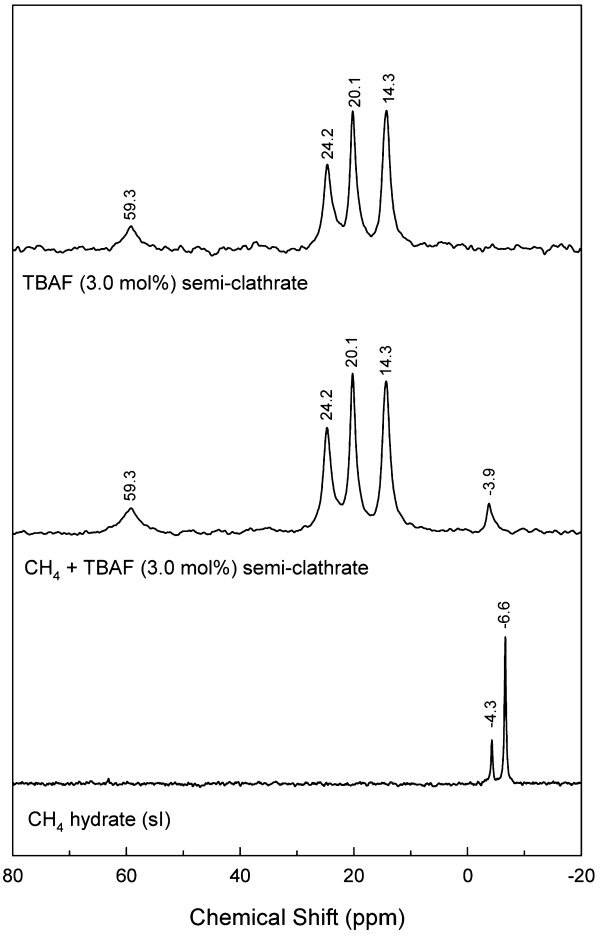

Figure 7. ^{13}C NMR spectra of the pure TBAF (3.0 mol %) semiclathrate, double CH_4 + TBAF (3.0 mol %) semiclathrate, and CH_4 hydrate.

TBAF (3.0 mol %) and double CH_4 + TBAF (3.0 mol %) semiclathrates was the same as each corresponding chemical shift from the pure TBAF (3.3 mol %) and double CH_4 + TBAF (3.3 mol %) semiclathrates even though the crystal structures of the TBAF·29.7 H_2O (3.3 mol %) semiclathrate and TBAF·32.8 H_2O (3.0 mol %) semiclathrate were reported to be cubic and tetragonal, respectively.[18,19,21,22] The cage-dependent ^{13}C NMR chemical shifts can be useful in confirming the enclathration of guest gas molecules in the double TBAF semiclathrates. However, ^{13}C NMR spectra are insufficient to identify each crystal structure of the TBAF semiclathrates formed at two different concentrations (3.0 and 3.3 mol %). Therefore, more sophisticated and advanced analysis methods are needed to reveal the accurate structural details of the double TBAF semiclathrates. From the overall ^{13}C NMR results, it can be concluded that the CH_4 molecules are captured in the 5^{12} cages of the double CH_4 + TBAF semiclathrates.

Raman spectroscopy, known to be simpler and less resource intensive,[35] was also used to examine the guest gas enclathration in the double TBAF semiclathrates. Figure 8

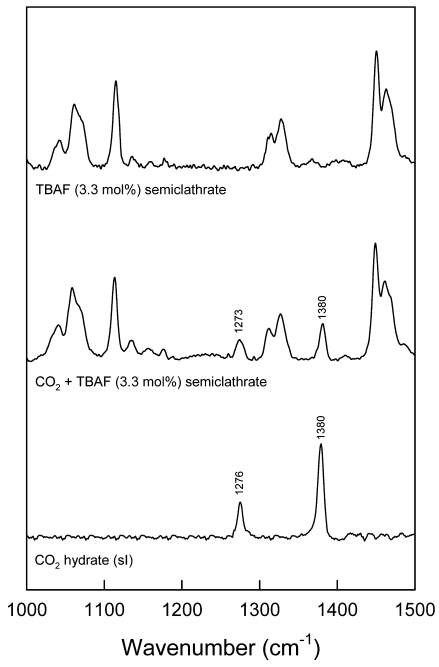

Figure 8. Raman spectra of the pure TBAF (3.3 mol %) semiclathrate, double CO_2 + TBAF (3.3 mol %) semiclathrate, and CO_2 hydrate.

shows a stacked plot of the Raman spectra of the CO_2 hydrate, pure TBAF (3.3 mol %) semiclathrate, and double CO_2 + TBAF (3.3 mol %) semiclathrate. In the pure CO_2 hydrate, when the CO_2 molecules are incorporated into the gas hydrate lattices of the sI, the two major bands, called the Fermi diad, were very pronounced at 1276 and 1380 cm^{-1}.[36] The positions of Raman peaks for the pure CO_2 hydrate are identical to those of literature reports.[17,36] However, unlike the NMR spectrum of the pure CH_4 hydrate, each of these two Raman peaks does not directly correspond to each small and large cage occupied by the CO_2 molecules even though the CO_2 molecules occupy both the small and large cages of sI. In the CO_2 + TBAF semiclathrate, peaks from the CO_2 molecules enclathrated in the double semiclathrate were shown at 1273 and 1380 cm^{-1}, and many other peaks from TBA^+ appeared at a wide range of wavenumbers. As was observed in the double CO_2 + TBAB semiclathrate,[17] a slight peak shift (1276 cm^{-1} → 1273 cm^{-1}) due to the structure transition of the sI to double semiclathrate was also detected in the double CO_2 + TBAF semiclathrate. However, more accurate information on the CO_2 enclathration behavior in the cages of the double CO_2 + TBAF semiclathrate could not be obtained because the Raman spectra for the CO_2 hydrate do not show peak splittings for guests in different cages.[8,17]

In the present study, the stability conditions, gas uptake characteristics, and guest gas enclathration behavior of the double TBAF semiclathrates with a guest gas (CH_4 or CO_2)

dx.doi.org/10.1021/jp302647c | J. Phys. Chem. B 2012, 116, 9075−9081

were investigated. Even though the presence of TBAF can offer greatly enhanced thermal stability, the amount of guest gas captured in the lattices of the double semiclathrate structure was found to be much lower than that of the pure CH_4 or CO_2 hydrate.

CONCLUSIONS

The three-phase (H−L_W−V) equilibria of the double TBAF semiclathrates with a guest gas (CH_4 or CO_2) were experimentally measured in order to determine the stability conditions. The double TBAF semiclathrates demonstrated greatly stabilized and shifted H−L_W−V equilibrium conditions represented by higher temperature and lower pressure regions when compared with the pure CH_4 (or CO_2) hydrate. The highest stabilization effect in the double semiclathrates was observed at the stoichiometric concentration corresponding to the hydration number of the pure TBAF semiclathrate, which is 3.3 mol %. The dissociation temperature and dissociation enthalpy of the pure TBAF semiclathrate were also confirmed via DSC. In addition, the gas uptake measurements were performed in order to estimate the guest gas amount consumed during the double semiclathrate formation. From the gas uptake experiment, CH_4 was found to be the more favorable guest gas to be enclathrated in the 5^{12} cages of the double TBAF semiclathrate compared with CO_2. From the NMR and Raman spectroscopic results, it was identified that the guest gas molecules (CH_4 or CO_2) were captured in the 5^{12} cages of the double TBAF semiclathrates. The overall experimental results from the stability condition determination, gas uptake measurement, and spectroscopic analysis examined in the present study are very helpful in understanding guest−host interactions and guest gas enclathration characteristics in the double semiclathrates and, thus, could be applied as valuable information in gas storage and separation using semiclathrates.

AUTHOR INFORMATION

Corresponding Author

*Tel +82-52-217-2821; Fax +82-52-217-2819; e-mail ywseo@unist.ac.kr.

Notes

The authors declare no competing financial interest.

ACKNOWLEDGMENTS

This work was supported by the Energy Efficiency & Resources Program of the Korea Institute of Energy Technology Evaluation and Planning (KETEP) grant funded by the Ministry of Knowledge Economy of Korea and also by Basic Science Research Program through the National Research Foundation of Korea (NRF) funded by the Ministry of Education, Science and Technology (2012-002494). This work was also supported by the year of 2012 Research Fund (1.110058.01) and the Creativity and Innovation Project (1.120022.01) of the UNIST (Ulsan National Institute of Science and Technology).

REFERENCES

(1) Sloan, E. D.; Koh, C. A. *Clathrate Hydrates of Natural Gases*, 3rd ed.; CRC Press: Boca Raton, FL, 2008.
(2) Lee, H.; Lee, J.-w.; Kim, D. Y.; Park, J.; Seo, Y. T.; Zeng, H.; Moudrakovski, I. L.; Ratcliffe, C. I.; Ripmeester, J. A. *Nature* **2005**, *434*, 743−746.
(3) Sugahara, T.; Haag, J. C.; Warntjes, A. A.; Prasad, P. S.; Sloan, E. D.; Koh, C. A.; Sum, A. K. *J. Phys. Chem. C* **2010**, *114*, 15218−15222.
(4) Takahashi, M.; Moriya, H.; Katoh, Y.; Iwasaki, T. Proceedings of the 6th International Conference on Gas Hydrates, Vancouver, Canada, July 6−10, 2008.
(5) Kang, S. P.; Lee, H. *Environ. Sci. Technol.* **2000**, *34*, 4397−4400.
(6) Seo, Y.; Kang, S. P. *Chem. Eng. J.* **2010**, *161*, 308−312.
(7) Linga, P.; Kumar, R.; Englezos, P. *Chem. Eng. Sci.* **2007**, *62*, 4268−4276.
(8) Kumar, R.; Englezos, P.; Moudrakovski, I.; Ripmeester, J. A. *AIChE J.* **2009**, *55*, 1584−1594.
(9) Seo, Y. T.; Moudrakovski, I. L.; Ripmeester, J. A.; Lee, J. W.; Lee, H. *Environ. Sci. Technol.* **2005**, *39*, 2315−2319.
(10) Lipkowski, J.; Komarov, V. Y.; Rodionova, T.; Dyadin, Y. A.; Aladko, L. S. *J. Supramol. Chem.* **2002**, *2*, 435−439.
(11) Aladko, L. S.; Dyadin, Y. A.; Rodionova, T. V.; Terekhova, I. S. *J. Struct. Chem.* **2002**, *43*, 990−994.
(12) Shimada, W.; Shiro, M.; Kondo, H.; Takeya, S.; Oyama, H.; Ebinuma, T.; Narita, H. *Acta Crystallogr., Sect. C: Cryst. Struct. Commun.* **2005**, *C61*, o65−o66.
(13) Chapoy, A.; Anderson, R.; Tohidi, B. *J. Am. Chem. Soc.* **2007**, *129*, 746−747.
(14) Hashimoto, S.; Sugahara, T.; Moritoki, M.; Sato, H.; Ohgaki, K. *Chem. Eng. Sci.* **2008**, *63*, 1092−1097.
(15) Kamata, Y.; Oyama, H.; Shimada, W.; Ebinuma, T.; Takeya, S.; Uchida, T.; Nagao, J.; Narita, H. *Jpn. J. Appl. Phys.* **2004**, *43*, 362−365.
(16) Duc, N. H.; Chauvy, F.; Herri, J. H. *Energy Convers. Manage.* **2007**, *48*, 1313−1322.
(17) Lee, S.; Park, S.; Lee, Y.; Lee, J.; Lee, H.; Seo, Y. *Langmuir* **2011**, *27*, 10597−10603.
(18) McMullan, R. K.; Bonamico, M.; Jeffrey, G. A. *J. Chem. Phys.* **1963**, *39*, 3295−3310.
(19) Dyadin, Yu. A.; Udachin, K. A. *J. Inclusion Phenom. Macrocyclic Chem.* **1984**, *2*, 61−72.
(20) Fan, S.; Li, S.; Wang, J.; Lang, X.; Wang, Y. *Energy Fuels* **2009**, *23*, 4202−4208.
(21) Komarov, V, Y.; Rodionova, T. V.; Terekhova, I. S.; Kuratieva, N. V. *J. Inclusion Phenom. Macrocyclic Chem.* **2007**, *59*, 11−15.
(22) Rodionova, T. V.; Manakov, A. Y.; Stenin, Y. G.; Villevald, G. V.; Karpova, T. D. *J. Inclusion Phenom. Macrocyclic Chem.* **2008**, *61*, 107−111.
(23) Aladko, E. Y.; Larionov, E. G.; Rodionova, T. V.; Aladko, L. S.; Manakov, A. Y. *J. Inclusion Phenom. Macrocyclic Chem.* **2010**, *68*, 381−386.
(24) Lee, S.; Lee, Y.; Park, S.; Seo, Y. *J. Chem. Eng. Data* **2010**, *55*, 5883−5886.
(25) Sakamoto, J.; Hashimoto, S.; Tsuda, T.; Sugahara, T.; Inoue, Y.; Ohgaki, K. *Chem. Eng. Sci.* **2008**, *63*, 5789−5794.
(26) Smith, J. M.; Van Ness, H. C.; Abbott, M. M. *Introduction to Chemical Engineering Thermodynamics*, 7th ed.; McGraw-Hill: New York, 2005.
(27) Lee, S.; Cha, I.; Seo, Y. *J. Phys. Chem. B* **2010**, *114*, 15079−15084.
(28) Cha, I.; Lee, S.; Lee, J. D.; Lee, G. W.; Seo, Y. *Environ. Sci. Technol.* **2010**, *44*, 6117−6122.
(29) Seo, Y.; Lee, H. *J. Phys. Chem. B* **2002**, *106*, 9668−9673.
(30) Adisasmito, S.; Frank, R. J.; Sloan, E. D. *J. Chem. Eng. Data* **1991**, *36*, 68−71.
(31) Li, S.; Fan, S.; Wang, J.; Lang, X.; Wang, Y. *J. Chem. Eng. Data* **2010**, *55*, 3312−3215.
(32) Takeya, S.; Udachin, K. A.; Moudrakovski, I. L.; Susilo, R.; Ripmeester, J. A. *J. Am. Chem. Soc.* **2010**, *132*, 524−531.
(33) Ripmeester, J. A.; Ratcliffe, C. I. *J. Struct. Chem.* **1999**, *40*, 654−662.
(34) Pavia, D. L.; Lampman, G. M.; Kriz, G. S.; Vyvyan, J. *Introduction to Spectroscopy*, 4th ed.; Brooks/Cole: Belmont, 2009.
(35) Uchida, T.; Hirano, T.; Ebinuma, T.; Narita, H.; Gohara, K.; Mae, S.; Matsumoto, R. *AIChE J.* **1999**, *45*, 2641−2645.
(36) Sum, A. K.; Burruss, R. C.; Sloan, E. D. *J. Phys. Chem. B* **1997**, *101*, 7371−7377.